PHYSICAL REVIEW D **80,** 023532 (2009)

Multiparameter investigation of gravitational slip

Scott F. Daniel,[1,*] Robert R. Caldwell,[1] Asantha Cooray,[2] Paolo Serra,[2] and Alessandro Melchiorri[3]

[1]*Department of Physics and Astronomy, Dartmouth College, Hanover, New Hampshire 03755, USA*

[2]*Department of Physics and Astronomy, University of California, Irvine, California 92697, USA*

[3]*Physics Department and Sezione INFN, University of Rome, "La Sapienza," Piazzale Aldo Moro 2, 00185 Rome, Italy*

(Received 17 January 2009; published 29 July 2009)

A detailed analysis of gravitational slip, a new post-general relativity cosmological parameter characterizing the degree of departure of the laws of gravitation from general relativity on cosmological scales, is presented. This phenomenological approach assumes that cosmic acceleration is due to new gravitational effects; the amount of spacetime curvature produced per unit mass is changed in such a way that a universe containing only matter and radiation begins to accelerate as if under the influence of a cosmological constant. Changes in the law of gravitation are further manifest in the behavior of the inhomogeneous gravitational field, as reflected in the cosmic microwave background, weak lensing, and evolution of large-scale structure. The new parameter ϖ_0 is naively expected to be of order unity. However, a multiparameter analysis, allowing for variation of all of the standard cosmological parameters, finds that $\varpi_0 = 0.09^{+0.74}_{-0.59}(2\sigma)$, where $\varpi_0 = 0$ corresponds to a cosmological constant plus cold dark matter universe under general relativity. Future probes of the cosmic microwave background (Planck) and large-scale structure (Euclid) may improve the limits by a factor of 4.

DOI: 10.1103/PhysRevD.80.023532 PACS numbers: 98.80.Es, 04.50.Kd, 98.65.Dx

I. INTRODUCTION

Cosmic acceleration [1,2] can be caused by new fluids, new theories of gravity, or some admixture of both [3]. This uncertainty places a premium on descriptions of the so-called "dark physics" which remain useful across different models and in spite of varying assumptions. In the case of new fluids (dark energy), the literature chooses to speak in terms of the equation of state w and its derivative [4]. In the case of new gravitational physics, the model-independent *lingua franca* is the relationship between the Newtonian (ψ) and longitudinal (ϕ) gravitational potentials. The potentials, implicitly defined through the perturbed Robertson-Walker metric

$$ds^2 = a^2[-(1+2\psi)d\tau^2 + (1-2\phi)d\vec{x}^2], \qquad (1)$$

are most familiar for their roles in Newton's equation $\ddot{\vec{x}} = -\vec{\nabla}\psi$ and the Poisson equation $\nabla^2\phi = 4\pi G a^2 \delta\rho$ under general relativity (GR).

The gravitational potentials are equal in the presence of nonrelativistic stress energy under GR. Alternate theories of gravity make no such guarantee. Scalar-tensor [5,6] and $f(R)$ theories [7–9], braneworld scenarios such as Dvali-Gabadadze-Porrati gravity [10–12], and massive gravity [13,14] all predict a systematic difference or "slip," so that $\phi \neq \psi$ in the presence of nonrelativistic stress energy. Efforts to develop a parametrized-post-Friedmannian (PPF) framework to phenomenologically describe this behavior are just as prolific: Refs. [15–24] all offer parametrizations quantifying the departure from $\phi = \psi$ due to new gravitational effects. We choose to work with the parametrization proposed in Ref. [16]:

$$\psi = [1 + \varpi(z)]\phi, \qquad (2)$$

$$\varpi(z) = \varpi_0(1+z)^{-3}. \qquad (3)$$

We assume the existence of a theory of gravitation that leads to an expansion history that is indistinguishable from that produced by a spatially-flat, cosmological constant plus cold dark matter (ΛCDM) scenario with density parameters Ω_m and $\Omega_\Lambda = 1 - \Omega_m$. This assumption is not essential, but it allows our analysis to focus solely on PPF effects. Our naive expectation is that $\varpi \simeq \Omega_\Lambda/\Omega_m$ by today. [Note that we have changed our notation, having previously defined $\varpi(z) = \varpi_0(\Omega_\Lambda/\Omega_m)(1+z)^{-3}$.]

The departure from GR kicks in only when the cosmic expansion begins to accelerate. Daniel *et al.* (hereafter DCCM) [22] discuss the compatibility with other parametrizations (especially that of Ref. [23]) and compare the implications of $\varpi_0 \neq 0$ to data from the Wilkinson Microwave Anisotropy Probe (WMAP) [25], the Canada-France-Hawaii Telescope Legacy Survey (CFHTLS) [26], and various galaxy surveys [27–29]. We expand upon their analysis in this work by performing a full likelihood analysis of the cosmological parameter space.

The previous work by DCCM considered the effects of modified gravity on cosmological perturbations in a one-parameter context: i.e., "how does the new (modified gravity) parameter affect cosmological data when all other parameters are held fixed (at the WMAP 3 yr maximum likelihood values)?" They used a modified version of the Boltzmann code CMBFAST [30] to evaluate the effect of ϖ_0 on the cosmic microwave background (CMB) anisotropy, matter power spectrum, weak lensing convergence corre-

*scott.f.daniel@dartmouth.edu

lation function, and galaxy-CMB cross-correlation power spectrum. While this analysis was useful for testing for the existence of PPF effects, the results glossed over degeneracies that exist between ϖ_0 and traditional cosmological parameters. Figure 9 of Ref. [22] already demonstrates a potential degeneracy between ϖ_0 and σ_8. Identifying further degeneracies and more rigorously motivating the possibility of nonzero ϖ_0 requires analysis across the full cosmological parameter space.

In the following, we present the results of a likelihood analysis based on a Monte Carlo Markov chain sampling of the space of cosmological parameters. The parameters, $\{\Omega_b h^2, \Omega_c h^2, \theta, \tau_{\rm ri}, n_s, A_s, A_{\rm SZ}, \varpi_0\}$, are, respectively, the baryon density, cold dark matter density, the ratio of the sound horizon to the angular diameter distance, the optical depth to last scattering, the scalar spectral index, the amplitude of the primordial curvature perturbations, and a normalization parameter for the Sunyaev-Zeldovich effect. These are the standard parameters in the convention used by the publicly-available code COSMOMC [31].

We generate our Markov chains using COSMOMC [32–34] with modules added to calculate likelihoods based on the weak lensing [35,36] and galaxy-CMB cross-correlation spectra [37]. The CMB data and likelihood code come from the WMAP team's 5 yr release [38]. Supernova data come from the Union data set produced by the Supernova Cosmology Project [39]. The weak lensing data come from the CFHTLS weak lensing survey [26,40].

To help understand our results, we present a closed system of ordinary differential equations describing the evolution of ϕ and the matter overdensity δ under $\varpi_0 \neq 0$. These results imply a correction to the Poisson equation that was neglected by DCCM. Section II presents these equations and uses them to describe the dependence of the large-angle CMB anisotropy on ϖ_0. Section III discusses the modifications made to the public COSMOMC codes to implement Eq. (2). Section IV presents the likelihood contours found from our Markov chains. Section V makes an attempt at forecasting the results of future experiments. We conclude in Sec. VI.

II. EVOLUTION OF PERTURBATIONS

The procedure for evolving the matter and metric perturbations is as follows. We assume that the perturbed stress-energy tensors for all matter and radiation are conserved independently of the theory of gravitation:

$$\nabla_\mu T^{\mu\nu} = 0. \tag{4}$$

We next impose the relationship given by Eq. (2) between potentials ϕ and ψ, which upon translation into the synchronous gauge implies an evolution equation for the metric variable $\alpha \equiv (\dot{h} + 6\dot{\eta})/2k^2$:

$$\dot{\alpha} = -(2 + \varpi)\mathcal{H}\alpha + (1 + \varpi)\eta - 12\pi G a^2(\bar{\rho} + \bar{p})\sigma/k^2. \tag{5}$$

Here, a dot indicates the derivative with respect to conformal time, h and η are the synchronous-gauge metric perturbations, $\mathcal{H} = \dot{a}/a$ is the conformal-time Hubble parameter, and σ is the shear in a fluid with mean density $\bar{\rho}$ and pressure $\bar{p}$. (We use the same notation as Ref. [41].) We further assume that there is no preferred reference frame introduced by the new gravitational effects; there is no "dark fluid" momentum flux or velocity relative to the dark matter and baryon cosmic rest frame. This condition is imposed by enforcing the same perturbed time-space equation as in GR,

$$k^2\dot{\eta} = 4\pi G a^2(\bar{\rho} + \bar{p})\theta, \tag{6}$$

where θ is the divergence of the velocity field in a fluid with mean density $\bar{\rho}$ and pressure $\bar{p}$. Satisfying this equation automatically means that Bertschinger's consistency condition, that long-wavelength curvature perturbations should evolve like separate Robertston-Walker spacetimes, is satisfied [15]. The model of $\varpi(z)$ plus the three Eqs. (4)–(6) close the system of equations. (See Refs. [16,22] for further details.) In order to study the late-time behavior of the system of equations, we may neglect the shear and velocity perturbations and express the evolution equations in conformal-Newtonian/longitudinal gauge as

$$\ddot{\phi} = -(3 + \varpi)\mathcal{H}\dot{\phi} - \dot{\varpi}\mathcal{H}\phi - (1 + \varpi)(\mathcal{H}^2 + 2\dot{\mathcal{H}})\phi, \tag{7}$$

$$\dot{\delta} = 3\dot{\phi} - \left(\frac{k}{\mathcal{H}}\right)^2 \frac{\dot{\phi} + (1 + \varpi)\mathcal{H}\phi}{1 - \dot{\mathcal{H}}/\mathcal{H}^2}, \tag{8}$$

where δ is the matter density contrast.

Consider the behavior of an overdense region $\delta > 0$ as it evolves from early times when GR is valid to late times when new gravitational effects characterized by ϖ become important. At early times, when the Poisson equation is valid, $\phi < 0$ for the overdensity. While the expansion is matter dominated, the potential remains static. However, at late times, with the onset of cosmic acceleration, the potential begins to evolve. In the case of GR, $\dot{\phi} > 0$ so the potential is stretched shallower. The density contrast δ continues to grow via gravitational instability, although the rate of growth is slowed. The evolution of ϕ can be understood in terms of a competition between the expansion diluting the matter density and stretching ϕ shallower, and the accretion of matter sourcing and deepening ϕ. In GR, the accelerated expansion upsets the balance in favor of dilution, so that ϕ becomes shallower and δ grows more slowly. When $\varpi_0 \neq 0$, the competition between effects changes. Numerically integrating Eqs. (7) and (8), we find that $\varpi_0 > 0$ causes ϕ to become even shallower, yet the density contrast grows faster, as illustrated in Figs. 1

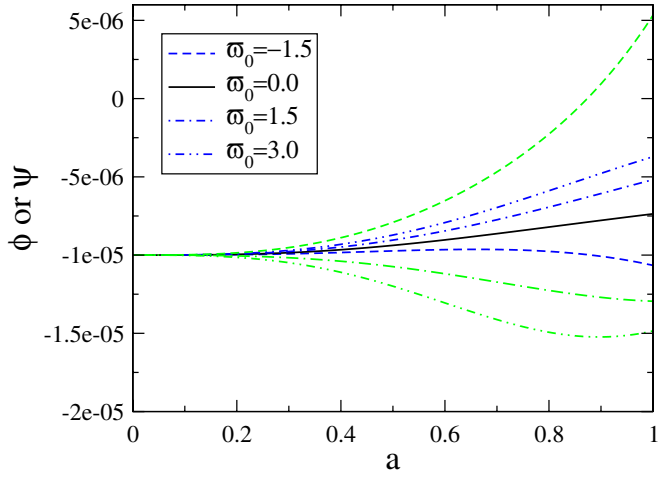

FIG. 1 (color online). The potentials ϕ and ψ are shown versus the scale factor, for different values of ϖ_0. The blue, dark curves are ϕ, whereas the green, light curves are ψ. Note that they behave oppositely; when ϕ becomes shallower, ψ becomes deeper, and vice versa.

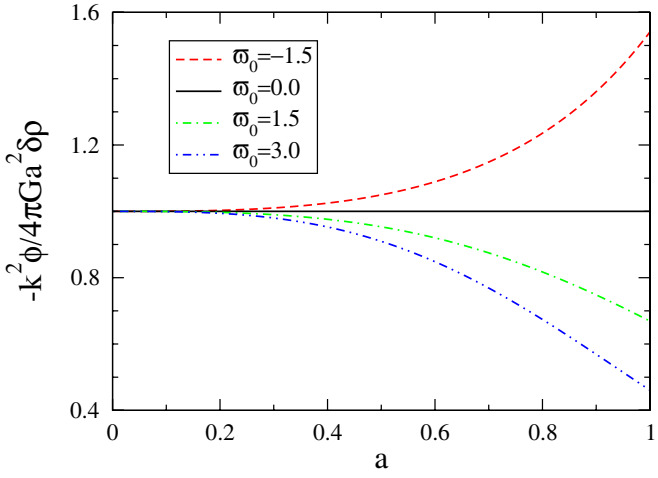

FIG. 3 (color online). The degree of deviation from the Poisson equation versus scale factor is shown for different values of ϖ_0. Because ϖ is scale independent, so too is the ratio $-k^2\phi/(4\pi G a^2 \delta\rho)$. For positive (negative) ϖ_0, a given ϕ corresponds to a larger (smaller) density contrast than in GR.

and 2. This seems counterintuitive, since the shallower potential should provide weaker attraction for the accretion of surrounding matter. In the case $\varpi_0 < 0$, the potential ϕ becomes more negative or deeper, and the density contrast grows more slowly. Likewise, the deeper potential should provide greater attraction. But here the difference between ϕ and ψ is important. As seen in Fig. 1, the potential ϕ grows shallower (deeper) for $\varpi_0 > 0$ (< 0). However, the potential responsible for geodesic motion $\psi = (1 + \varpi)\phi$ behaves oppositely, becoming deeper (shallower). Hence, the competition swings in favor of increased clustering over dilution by the expansion.

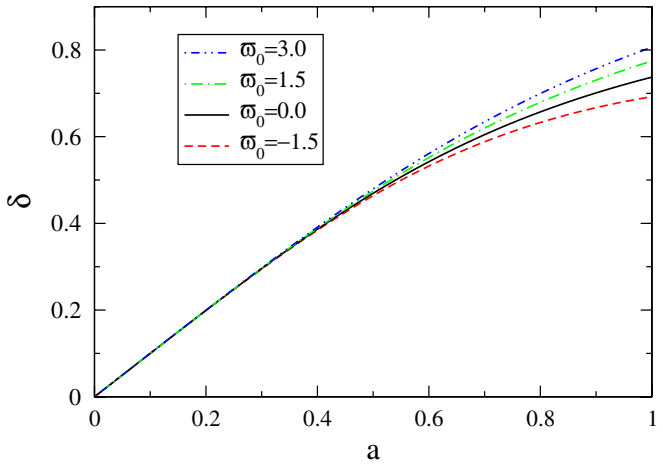

FIG. 2 (color online). The matter density contrast is shown versus the scale factor, for different values of ϖ_0. The time evolution is obtained by integrating Eqs. (7) and (8), with initial conditions $\phi = -10^{-5}$, $\dot{\phi} = 0.0$ for $k = 0.01$ Mpc^{-1}. Positive (negative) values of ϖ_0 enhance (slow) the growth of density perturbations.

The new behavior of ϕ and δ implies a correction to the Poisson equation. As seen in Fig. 3, for $\varpi_0 > 0$ (< 0), the density contrast grows more (less) rapidly, and the potential ϕ becomes shallower (deeper), so that the ratio

$$\Gamma \equiv -k^2\phi/(4\pi G a^2 \delta\rho) \tag{9}$$

grows smaller (larger). This suggests that we can restore the Poisson equation by introducing a time-dependent gravitational constant $G_{\rm eff} = G\Gamma$, whence $-k^2\phi = 4\pi G_{\rm eff} a^2 \delta\rho$. Note that $G_{\rm eff}$ is not a free function, but is determined by Eqs. (4)–(6). Because we have chosen ϖ to be scale independent, $G_{\rm eff}$ is too. A different strategy, whereby the time and space dependence of $G_{\rm eff}$ is imposed separately [20], will not necessarily satisfy Eqs. (4)–(6).

We can use this new understanding to explain the curious behavior of the large-angular scale CMB anisotropy spectrum. The effect of $\varpi_0 \neq 0$ on the low l moments of the CMB anisotropy is not monotonic, as seen in Fig. 4. The cause is the suppression of the integrated Sachs-Wolfe effect (ISW) at $\varpi_0 \simeq 1$. If the gravitational potentials in the Universe are evolving with time, then CMB photons will lose less (more) energy climbing out of potential wells than they gained falling in, resulting in a net blueshift (redshift) as the potentials shrink (grow). This is the ISW effect whereby time-evolving gravitational potentials contribute to the moments of the photon distribution function $\Theta_l(k, \eta)$ via

$$\int_0^{\tau_0} d\tau(\dot{\phi}(k,\tau) + \dot{\psi}(k,\tau)) j_l(k(\tau_0 - \tau)) \exp[-\tau_{\rm ri}(z)]. \tag{10}$$

(See Eq. (8.55) of Ref. [42].) Here j_l is a spherical Bessel function of the first kind, τ is the conformal time, τ_0 is the conformal time at $z = 0$, and $\tau_{\rm ri}(z)$ is the optical depth to

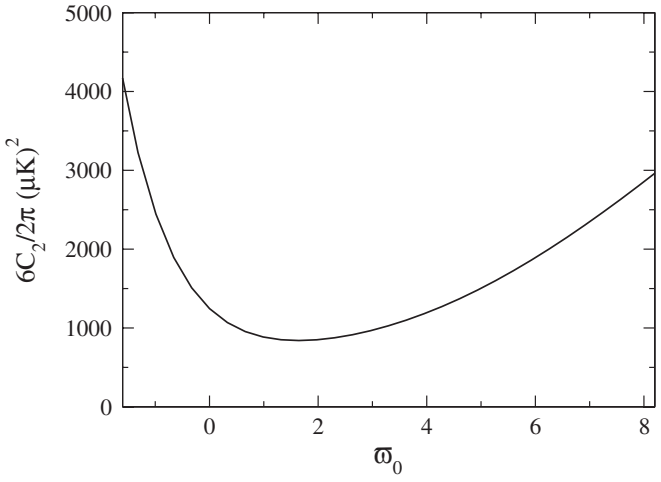

FIG. 4. The CMB quadrupole moment is shown versus ϖ_0. As explained in the text, the quadratic dependence can be understood in terms of the influence of ϖ_0 on the ISW effect. [Reproduced from Ref. [22] with our new normalization Eq. (3).]

redshift z. The strength of the ISW effect is determined by the sum $\dot{\phi} + \dot{\psi}$, which, using Eqs. (2) and (3), is given by

$$\dot{\phi} + \dot{\psi} = \dot{\phi}(2 + \varpi) + \phi\dot{\varpi} = \dot{\phi}(2 + \varpi) + 3\phi\mathcal{H}\varpi. \tag{11}$$

Again consider the evolution of an overdensity $\delta > 0$ with $\phi < 0$. In GR, the sum is positive, $\dot{\phi} + \dot{\psi} > 0$. When $\varpi_0 < 0$, the second term in Eq. (11) is always positive. The first term is generally subdominant, since $|\dot{\phi}| < |\mathcal{H}\phi|$, as can be inferred from Fig. 5. Therefore $\varpi_0 < 0$ enhances the ISW effect. When $\varpi_0 > 0$, there is a competition between the first and second terms; the first term is positive, whereas the second term is negative. The first term always wins, but at some intermediate value of ϖ_0 the two terms nearly cancel, thereby suppressing the ISW effect relative to the case with $\varpi_0 = 0$. This explains the dip in the quadrupole moment versus ϖ_0, as seen in Fig. 4.

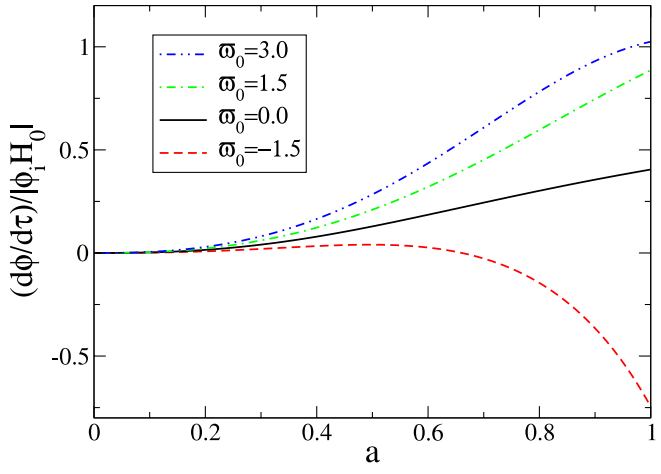

FIG. 5 (color online). The conformal-time derivative of the gravitational potential ϕ is shown versus the scale factor, for different values of ϖ_0. Initial conditions are the same as in Fig. 2. The potential well is decaying when $\frac{d\phi}{d\tau}/|\phi_i H_0| > 0$ and is deepening when negative.

III. IMPLEMENTATION

The modifications of the Monte Carlo Markov chain software COSMOMC to allow for $\varpi_0 \neq 0$ proceed almost identically to the modifications made to CMBFAST by DCCM, with a few differences. To compare the predictions of our model with weak lensing data, we adapt the weak lensing module provided by Refs. [35,36]. We modify it to assess the likelihood in terms of the variance of the aperture mass [Eq. (5) of [26]] with a full covariance matrix [43]. Because we probe weak lensing at nonlinear scales, we calculate the power spectrum of the lensing potential by extrapolating the linear matter power spectrum P_δ to nonlinear scales and using the relationship (9) between the matter overdensity δ and the gravitational potential ϕ to find the nonlinear P_ϕ. Whereas CMBFAST calculates the nonlinear matter power spectrum from the phenomenological fit of Peacock and Dodds [44], COSMOMC (having been built around the code CAMB [33]) uses the fit by Smith *et al.* [45] (see their Appendix C). Smith *et al.* express their fit as a nontrivial function of the linear power spectrum and Ω_m. This function assumes the ΛCDM relationship between Ω_m and perturbation growth. Gravitational slip alters this relationship, as discussed above in Sec. II. Therefore, to adapt the fit of Smith *et al.* to the case $\varpi_0 \neq 0$, we use the phenomenological relationship [see Eq. (24) of [22]]

$$\Omega_m|_{\varpi_0=0} = \Omega_m|_{\varpi_0\neq 0} + 0.13\varpi_0\frac{\Omega_m}{\Omega_\Lambda} \tag{12}$$

to find a $\varpi_0 = 0$, ΛCDM model with a similar growth history to our $\varpi_0 \neq 0$ model and use that value of $\Omega_m|_{\varpi_0=0}$ in Eq. (C18) of Smith *et al.*. Equation (12) breaks down for $\Omega_m|_{\varpi_0\neq 0} \leq 0.15$, but this region of parameter space is excluded to at least 2σ (see Fig. 6). A second COSMOMC run with a more accurate fitting function yielded identical results to those obtained using Eq. (12).

This is not a precise method for determining the nonlinear power spectrum in the presence of gravitational slip. Precision would require examination of N-body simulations which, unfortunately, implies assumptions about what alternative theory of gravity we are constraining. Recently, much work has been done attempting to calculate the nonlinear power spectrum directly, without the aid of an N-body simulation. Crocce and Scoccimarro propose to expand the nonlinear power spectrum as a Taylor-like sum,

$$P_\delta = \sum_i P_\delta^{(i)}, \tag{13}$$

where the different orders of P_δ are derived from a dia-

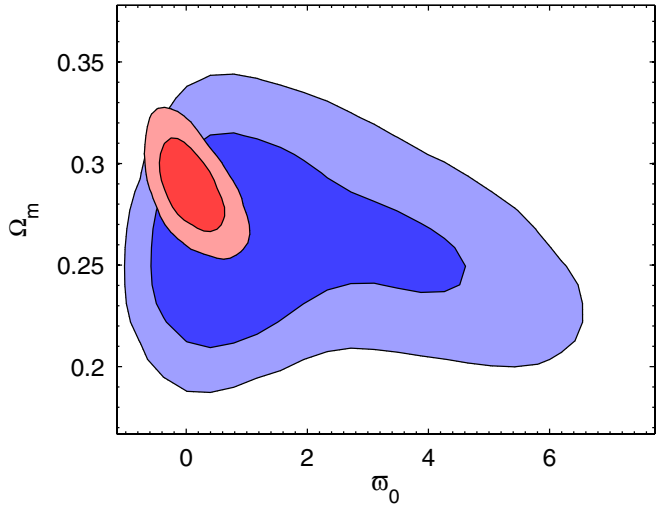

FIG. 6 (color online). The 68% and 95% likelihood contours in the $\varpi_0 - \Omega_m$ parameter space are shown. The broad, blue contours are based on CMB data alone. The smaller, red contours add weak lensing, type 1a supernovae and galaxy-CMB cross-correlation data.

grammatic scheme similar to Feynman diagrams [46]. They find that the resulting sum (13) is much better behaved than results derived from perturbation theory (see their Fig. 1). Matarrese and Pietroni [47] use the formalism of renormalization group theory to derive a generating functional for the different orders of P_δ. Taruya and Hiramatsu adapt methods from the statistical studies of fluid instabilities to separate out and solve for the cross-mode interactions in $\tilde{\delta}$ [48]. All of these methods yield better agreement with the results of N-body simulations than standard perturbation theory in the case of $\varpi = 0$ (see Fig. 2 of Ref. [49], Fig. 8 of Ref. [47], and Fig. 3 of Ref. [50]). Work has already begun adapting them to alternative gravity theories. In Ref. [51], Koyama, Taruya, and Hiramatsu extend the method of Ref. [48] to include $f(R)$ and Dvali-Gabadadze-Porrati gravity theories by assuming that they can be approximated with a Brans-Dicke scalar-tensor theory on subhorizon scales. Hiramatsu and Taruya [50] also try to encompass modified gravity theories by parametrizing them in terms of their implied effective Newton's constant $G_{\rm eff} = \Gamma G$ [see Eq. (14) of the present work]. Following their lead, it should be possible to adapt the nonlinear power spectrum calculations of Ref. [48]—or even [46,47]—to account for model-independent gravitational slip. Such a calculation is beyond the scope of this work. Given the relatively well-behaved regions of parameter space allowed by experiments (see Sec. IV below), we do not expect this limitation to significantly influence our findings.

To incorporate the galaxy-CMB cross correlation, we use the module written by Ho *et al.* [37]. Modifications for $\varpi_0 \neq 0$ enter as modifications to the $\phi + \psi$ power spectrum (see Sec. II of [37]),

$$P_{\phi+\psi} = \frac{9}{4}\Omega_{m,0}^2\left(\frac{H_0}{ck}\right)^4\left(\frac{D_\varpi}{a}\right)^2\left[\left(1+\frac{1}{2}\varpi\right)\Gamma\right]^2 \times P_\delta. \quad (14)$$

Note that Eq. (27) of Ref. [22] neglected the factor Γ, defined in Eq. (9), to correct the Poisson equation. The corrected weak lensing statistics show the same qualitative behavior as in Fig. 10 of Ref. [22]. However, large values of $|\varpi_0| \gg 1$ have a weaker effect on the amplitude of the convergence spectrum.

IV. RESULTS

The results of our multiparameter investigation are shown in Figs. 6 and 7. Figure 6 shows the 68% and 95% contours in (Ω_m, ϖ_0) space marginalized over all other parameters. Figure 7 shows the same contours in (σ_8, ϖ_0) space. Red (smaller) likelihood contours were generated using all available data sets (WMAP 5 yr [38], Supernova Union [39], CFHTLS [26], and the galaxy surveys selected by [37]). Blue (larger) contours were generated using only the WMAP 5 yr data. For each set of constraints, we generated four independent Markov chains. We achieved convergence by running the calculations until the statistic $|1 - R|$ was much less than unity, where R is Gelman and Rubin's potential scale reduction factor, defined as the ratio of the variance across all of the chains to the mean of the variance of each individual chain evaluated for the least converged parameter [31,52,53]. Our conclusions are three-fold:

(i) Present cosmological data constrains gravity to agree with GR, assuming the background evolution is consistent with ΛCDM.

(ii) Very negative values of ϖ_0 are ruled out. This should not be surprising, since a sign difference

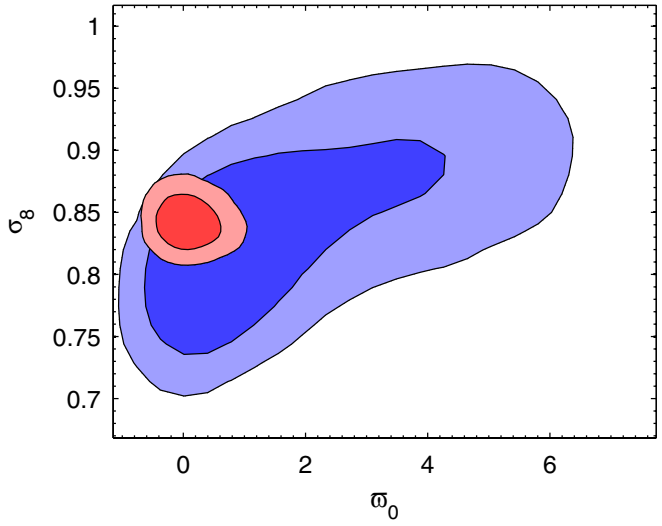

FIG. 7 (color online). The 68% and 95% likelihood contours in the $\varpi_0 - \sigma_8$ parameter space are shown. Shading is the same as in Fig. 6. Note that the addition of large-scale structure data breaks the degeneracy in $\varpi_0 - \sigma_8$.

TABLE I. Marginalized (1σ) constraints for cosmological parameters resulting from Monte Carlo Markov chain analysis. The left and center columns are generated using all available data sets (CMB, weak lensing, supernovae, and galaxy-CMB cross correlation). The left column is generated by marginalizing over ϖ_0. The center column fixes $\varpi_0 = 0$. Because our constraint on ϖ_0 is consistent with $\varpi_0 = 0$, we find little difference between the two columns. The right column shows the constraints reported by the WMAP team in Ref. [38] based on just the WMAP 5 yr data. The principal improvements from adding supernova, weak lensing, and galaxy-CMB cross-correlation data lie in constraining Ω_Λ (a result of adding the supernovae) and σ_8 (a result of adding weak lensing).

Parameter	$\varpi_0 \neq 0$	$\varpi_0 = 0$	WMAP 5 yr
$\Omega_b h^2$	$0.02262^{+0.00059}_{-0.00058}$	$0.02264^{+0.00058}_{-0.00057}$	0.02273 ± 0.00062
$\Omega_{\rm cdm} h^2$	0.1167 ± 0.0026	0.1170 ± 0.0016	0.1109 ± 0.0062
θ_s	$1.0417^{+0.0029}_{-0.0028}$	$1.0419^{+0.0028}_{-0.0029}$	1.0400 ± 0.0029
$\tau_{\rm ri}$	0.085 ± 0.016	$0.087^{+0.017}_{-0.016}$	0.087 ± 0.017
n_s	0.964 ± 0.014	0.965 ± 0.014	$0.963^{+0.014}_{-0.015}$
Ω_Λ	0.712 ± 0.014	$0.710^{+0.012}_{-0.011}$	0.742 ± 0.030
σ_8	0.842 ± 0.014	0.844 ± 0.015	0.796 ± 0.036
h	0.696 ± 0.014	0.695 ± 0.013	$0.719^{+0.026}_{-0.027}$

between the longitudinal and Newtonian gravitational potentials would mean that test particles are repelled by overdense regions.

(iii) Large-scale structure data (in our case, weak lensing and the galaxy-CMB correlation) are critical to constraining ϖ_0.

The effects described in Sec. II mean that any CMB anisotropy spectrum can be reasonably well approximated (modulo a normalization) by two possible values of ϖ_0. Figure 1 of Ref. [22] showed that $\varpi_0 \neq 0$ has no effect on the shape of higher l multipoles within linear theory. This explains the double-peaked likelihood curve in Fig. 3 of Ref. [22] and the broad blue contours in Figs. 6 and 7 in this work. Fortunately, the effect of $\varpi_0 \neq 0$ on cosmic structure is monotonic in the range of interest (as discussed by DCCM), so that only one value of ϖ_0 is maximally likely for any given realization of weak lensing and galaxy-CMB cross-correlation data, hence the smaller red contours in Figs. 6 and 7. Marginalizing over all other parameters, the WMAP 5 yr data alone give $\varpi_0 = 1.7^{+4.0}_{-2.0}(2\sigma)$. Supernovae, weak lensing, and the galaxy-CMB cross-correlation data improve the constraint to $\varpi_0 = 0.09^{+0.74}_{-0.59}(2\sigma)$. Table I presents the marginalized 1σ limits on the other cosmological parameters of note.

V. FORECASTS

It is useful to ask how much better our constraints will be under future experiments. We generate two mock data sets—one simulating the results of the upcoming Planck CMB experiment and the other simulating the results of a future weak lensing survey, modeled after the proposed European Space Agency experiment Euclid—and feed them into our modified COSMOMC.

To simulate Planck data, we use a fiducial model given by the best fit parameters of WMAP [38] with noise properties consistent with a combination of Planck 100-143-217 GHz channels of the high frequency instrument [54]; in this case we fit also for B modes produced by lensing of the CMB (see Ref. [55]), and we use the full-sky likelihood function given in [56].

To simulate weak lensing data, we generate a mock convergence power spectrum $P_\kappa(l)$ [Eq. (2) of Ref. [26]] corrected for alternative gravity as in Eq. (14). We generate data in bins of size $\Delta_l = 1$ for $2 \leq l < 100$ and $\Delta_l = 40$ for $100 < l < 2980$. We simulate the (1σ) errors as [Eq. (11) of Ref. [57]]

$$\sigma_l = \sqrt{(2/(2l+1))/(\Delta_l f_{\rm sky})}(P_\kappa(l) + \sigma_\epsilon^2/n_{\rm gal}),$$

taking $\sigma_\epsilon = 0.25$, $n_{\rm gal} = 35(\text{arc minute})^{-2}$ and $f_{\rm sky} = 0.48$, consistent with values projected for the European Space Agency's Euclid experiment (Table I of Ref. [58]). These assumptions will give us a tighter constraint than if we had used Supernova Acceleration Probe/Joint Dark Energy Mission parameters, since Supernova Acceleration Probe/Joint Dark Energy Mission has a smaller $f_{\rm sky}$ by a factor of 10 [59]. We fit the redshift distribution of sources $n(z)$ from a mock data set based on Eq. (14) of Ref. [26] with parameter values taken from their Table I. The 1σ errors in our mock $n(z)$ are reduced from actual values [43] by a factor of $1/\sqrt{2}$. The likelihood relative to the mock weak lensing data is calculated as a simple χ^2 (i.e., we assume that the covariance matrix is diagonal). This is a safe assumption according to [60]. Figures 8 and 9 show the resulting likelihood contours.

Looking at the long and narrow, Planck-only (yellow) contours, we see the weakness of using CMB measure-

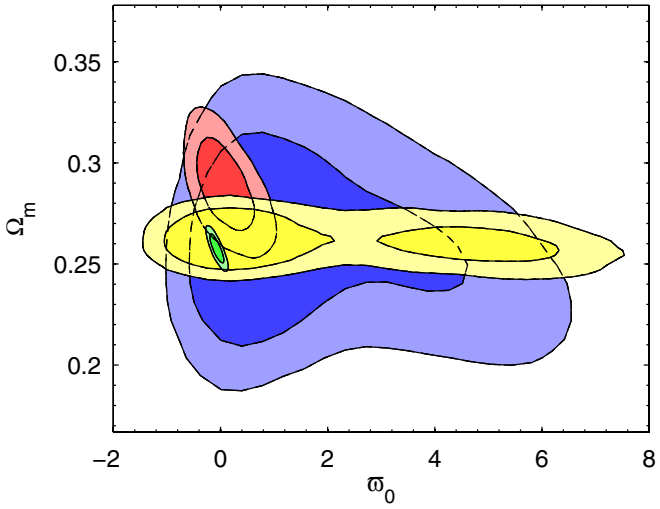

FIG. 8 (color online). The projected 68% and 95% likelihood contours in the $\varpi_0 - \Omega_m$ parameter space are shown. The long and narrow, yellow contours are based on mock Planck data. The tiny, green contours add mock weak lensing data. The underlying model is assumed to be $\varpi_0 = 0$ with $\Omega_m = 0.26$. The current constraints are shown for reference.

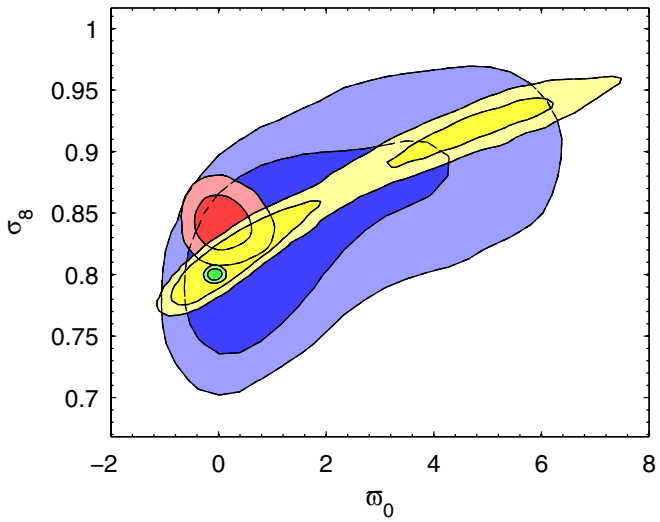

FIG. 9 (color online). The projected 68% and 95% likelihood contours in the $\varpi_0 - \sigma_8$ parameter space are shown. Shading is the same as in Fig. 8.

ments alone to constrain ϖ_0, as a bimodal distribution is obtained once again. We also see more clearly in Fig. 9 the degeneracy between ϖ_0 and σ_8 as normalization parameters (one can interpret the effect of ϖ_0 on δ in Fig. 2 as a renormalization of the matter power spectrum). Since weak lensing statistics depend sensitively on the power spectrum normalization, they once again break the degeneracy. Marginalizing over all other parameters, the mock data sets give the constraint $\varpi_0 = -0.07^{+0.13}_{-0.16}(2\sigma)$, a factor of $\sim$4 improvement over the current constraint.

VI. CONCLUSIONS

If we are justified in describing the background evolution by a ΛCDM universe, then the results illustrated in Figs. 6 and 7 do not appear to indicate a significant departure from GR. In fact, these results conflict with our naive expectation that $\varpi_0 \simeq \Omega_\Lambda/\Omega_m$. However, these results allow the ratio of ϕ to ψ to vary by order unity from the predictions of GR at the present epoch. (Weaker constraints yet result if the redshift dependence of $\varpi(z)$ is allowed to vary; see Ref. [55].) These are not very tight constraints. As shown in Sec. V, it seems likely that experiments already under consideration will give us much tighter constraints on parametrized-post-Friedmannian departures from GR in the near future. If, indeed, future constraints improve, we may need to reconsider the assumption of homogeneous ϖ.

Throughout this paper we neglect any possible scale dependence of ϖ. This simplifying assumption seems justified given the absence of any significant departure from GR. Were we to see evidence of a departure from GR, the onus would be on us to demonstrate the new theory's consistency with solar system-scale tests, all of which prefer GR to one part in 10^5 (e.g. Ref. [61]). Beyond this experimental evidence, we expect that ϖ should be scale dependent simply due to the differing evolution histories of sub- and super-horizon perturbation modes. Other work has already attempted to tackle this expectation. Hu and Sawicki implement a scale-dependent gravitational slip, based on the behavior seen in $f(R)$ models of gravity [18]. Afshordi *et al.* offer a scale-dependent parametrization of $-(\psi - \phi)/(\phi + \psi)$ designed to be consistent with higher-dimensional generalizations of Dvali-Gabadadze-Porrati gravity [62]. Though they find that their parametrization is capable of describing effects qualitatively consistent with tensions in current data sets, none of those tensions is strong enough to warrant a detection of alternative gravity. Koivisto and Mota explore a different set of new gravitational effects by supposing that dark energy is an imperfect (nonzero shear) fluid [63]. Shear σ, like gravitational slip, affects the space-space, off-diagonal perturbed Einstein equation, $k^2(\phi - \psi) = 12\pi G a^2 \bar{\rho}(1 + w)\sigma$. The imperfect fluid introduces a dark flow, however, so that the gravitational effects are not fully equivalent to the results of gravitational slip. Like the present work, they find that data cannot yet definitively rule in or out the interesting regions of their parameter space. Specifically, they find that the effect of nonzero shear on the CMB anisotropy spectrum is weaker than the effect of ϖ demonstrated by DCCM.

We have also shown that the modification of the Poisson equation follows uniquely from the assumptions of our model: the enforced relationship between ϕ and ψ, the conservation of stress energy, and the absence of a preferred frame indicated by a "dark flow." This must be

taken into account when conducting future tests of GR on cosmological scales.

ACKNOWLEDGMENTS

This work was supported by NSF CAREER AST-0349213 (R. C.) and AST-0645427 (A. C.). A. C. and R. C. thank Caltech for hospitality while this work was completed. The research of A. M. is supported by ASI Contract No. I/016/07/0 ''COFIS''.

[1] A. G. Riess *et al.* (Supernova Search Team Collaboration), Astron. J. **116**, 1009 (1998).
[2] S. Perlmutter *et al.* (Supernova Cosmology Project Collaboration), Astrophys. J. **517**, 565 (1999).
[3] J. P. Uzan, Gen. Relativ. Gravit. **39**, 307 (2007).
[4] A. Albrecht *et al.*, arXiv:astro-ph/0609591.
[5] S. M. Carroll, *An Introduction to General Relativity: Spacetime and Geometry* (Addison-Wesley, San Francisco, 2004), p. 513.
[6] C. Schimd, J. P. Uzan, and A. Riazuelo, Phys. Rev. D **71**, 083512 (2005).
[7] S. Capozziello, S. Carloni, and A. Troisi, in *Recent Research Developments in Astronomy and Astrophysics*, edited by S. G. Pandalai (Research Signpost, Trivandrum, India, 2003), Vol. 1, p. 625.
[8] V. Acquaviva, C. Baccigalupi, and F. Perrotta, Phys. Rev. D **70**, 023515 (2004).
[9] P. Zhang, Phys. Rev. D **73**, 123504 (2006).
[10] G. R. Dvali, G. Gabadadze, and M. Porrati, Phys. Lett. B **485**, 208 (2000).
[11] A. Lue, Phys. Rep. **423**, 1 (2006).
[12] Y. S. Song, I. Sawicki, and W. Hu, Phys. Rev. D **75**, 064003 (2007).
[13] S. L. Dubovsky, J. High Energy Phys. 10 (2004) 076.
[14] M. V. Bebronne and P. G. Tinyakov, Phys. Rev. D **76**, 084011 (2007).
[15] E. Bertschinger, Astrophys. J. **648**, 797 (2006).
[16] R. Caldwell, A. Cooray, and A. Melchiorri, Phys. Rev. D **76**, 023507 (2007).
[17] P. Zhang, M. Liguori, R. Bean, and S. Dodelson, Phys. Rev. Lett. **99**, 141302 (2007).
[18] W. Hu and I. Sawicki, Phys. Rev. D **76**, 104043 (2007).
[19] L. Amendola, M. Kunz, and D. Sapone, J. Cosmol. Astropart. Phys. 04 (2008) 013.
[20] B. Jain and P. Zhang, Phys. Rev. D **78**, 063503 (2008).
[21] P. Zhang, R. Bean, M. Liguori, and S. Dodelson, arXiv:0809.2836.
[22] S. F. Daniel, R. R. Caldwell, A. Cooray, and A. Melchiorri, Phys. Rev. D **77**, 103513 (2008).
[23] E. Bertschinger and P. Zukin, Phys. Rev. D **78**, 024015 (2008).
[24] W. Hu, Phys. Rev. D **77**, 103524 (2008).
[25] http://lambda.gsfc.nasa.gov
[26] L. Fu *et al.*, Astron. Astrophys. **479**, 9 (2008).
[27] E. Gaztanaga, M. Manera, and T. Multamaki, Mon. Not. R. Astron. Soc. **365**, 171 (2006).
[28] T. Giannantonio *et al.*, Phys. Rev. D **74**, 063520 (2006).
[29] A. Cabre, E. Gaztanaga, M. Manera, P. Fosalba, and F. Castander, Mon. Not. R. Astron. Soc. **372**, L23 (2006).
[30] U. Seljak and M. Zaldarriaga, Astrophys. J. **469**, 437 (1996).
[31] A. Lewis and S. Bridle, http://cosmologist.info/cosmomc/readme.html.
[32] A. Lewis and S. Bridle, http://cosmologist.info/notes/COSMOMC.ps.gz.
[33] A. Lewis, A. Challinor, and A. Lasenby, Astrophys. J. **538**, 473 (2000).
[34] A. Lewis and S. Bridle, Phys. Rev. D **66**, 103511 (2002).
[35] R. Massey *et al.*, arXiv:astro-ph/0701480.
[36] J. Lesgourgues, M. Viel, M. G. Haehnelt, and R. Massey, J. Cosmol. Astropart. Phys. 11 (2007) 008.
[37] S. Ho, C. Hirata, N. Padmanabhan, U. Seljak, and N. Bahcall, Phys. Rev. D **78**, 043519 (2008).
[38] J. Dunkley *et al.* (WMAP Collaboration), Astrophys. J. Suppl. Ser. **180**, 306 (2009).
[39] M. Kowalski *et al.*, Astrophys. J. **686**, 749 (2008).
[40] M. Kilbinger *et al.*, Astron. Astrophys. **497**, 677 (2009).
[41] C. P. Ma and E. Bertschinger, Astrophys. J. **455**, 7 (1995).
[42] S. Dodelson, *Modern Cosmology* (Academic Press, Amsterdam, Netherlands, 2003), p. 440.
[43] M. Kilbinger (private communication).
[44] J. A. Peacock and S. J. Dodds, Mon. Not. R. Astron. Soc. **280**, L19 (1996).
[45] R. E. Smith *et al.* (Virgo Consortium Collaboration), Mon. Not. R. Astron. Soc. **341**, 1311 (2003).
[46] M. Crocce and R. Scoccimarro, Phys. Rev. D **73**, 063519 (2006).
[47] S. Matarrese and M. Pietroni, J. Cosmol. Astropart. Phys. 06 (2007) 026.
[48] A. Taruya and T. Hiramatsu, arXiv:0708.1367.
[49] M. Crocce and R. Scoccimarro, Phys. Rev. D **77**, 023533 (2008).
[50] T. Hiramatsu and A. Taruya, Phys. Rev. D **79**, 103526 (2009).
[51] K. Koyama, A. Taruya, and T. Hiramatsu, Phys Rev. D **79**, 123512 (2009).
[52] A. Gelman and D. Rubin, Stat. Sci. **7**, 457 (1992).
[53] S. P. Brooks and A. Gelman, J. Comput. Graph. Stat. **7**, 434 (1998).
[54] G. Efstathiou, C. Lawrence, and J. Tauber, arXiv:astro-ph/0604069.
[55] P. Serra, A. Cooray, S. F. Daniel, R. Caldwell, and A. Melchiorri, Phys. Rev. D **79**, 101301(R) (2009).
[56] A. Lewis, Phys. Rev. D **71**, 083008 (2005).

[57] A. R. Cooray, Astron. Astrophys. **348**, 31 (1999).
[58] T. D. Kitching, A. F. Heavens, L. Verde, P. Serra, and A. Melchiorri, Phys. Rev. D **77**, 103008 (2008).
[59] http://snap.lbl.gov/.
[60] A. Cooray and W. Hu, Astrophys. J. **554**, 56 (2001).
[61] B. Bertotti, L. Iess, and P. Tortora, Nature (London) **425**, 374 (2003).
[62] N. Afshordi, G. Geshnizjani, and J. Khoury, arXiv:0812.2244.
[63] T. Koivisto and D. F. Mota, Phys. Rev. D **73**, 083502 (2006).